# ELECTRON BEAM PERFORATION AND JOINING OF METALLIC SUCTION SHEETS WITH PRE-APPLIED ADHESIVE TO CORE STRUCTURES IN HLFC SUCTION PANELS

Muhammad Anas Athar\*†, Shravani Patki\*, Sven Hartwig\* and Klaus Dilger\*

\* Institute of Joining and Welding, Technische Universität Braunschweig

Langer Kamp 8, 38106 Braunschweig

muhammad-anas.athar@tu-braunschweig.de

† Corresponding Author

#### Abstract

Hybrid Laminar Flow Control (HLFC) suction panels are employed in aircraft design to reduce drag and improve fuel efficiency, contributing to sustainable aviation. These panels feature suction surfaces with micro-perforations that draw air from the boundary layer, delaying the transition from laminar to turbulent flow and significantly reducing drag. A key challenge in HLFC panel design is preventing blockage of micro-holes. The perforation technique and the bonding method for joining suction surface to core are the critical factors. While laser drilling is commonly used, it is slow and generates thermal effects, leading to residual stresses, burning and damage of the surface. Electron beam drilling, in contrast, is faster and generates minimal heat, reducing the risk of damage to the surfaces. Also, the application of adhesive and bonding of suction surfaces after perforation leads to blockages of the microholes which has to be avoided. Hence, this study explores electron beam drilling of metallic facesheets pre-coated with aerospace-grade adhesive films. Two adhesive films are mechanically characterized for tensile and bonding strength using tensile and peel tests. The adhesives are applied to the metallic sheets, partially cured in a vacuumed autoclave or a heated oven and the metallic sheets are then perforated with electron beam drilling. Three types of Triply Periodic Minimal Surface (TPMS) cores namely gyroid, primitive and diamond are used. After perforation, bonding of the suction surfaces to the core structures takes place again in the autoclave. The sandwich panels are analyzed under a Scanning Electron Microscope (SEM) to evaluate micro-hole blockages and morphology. Flow meter tests are performed to assess airflow properties while compression tests determine the load-bearing capacities of the adhesives, TPMS cores and overall structural integrity of the panels. This approach aims to optimize HLFC panel design by addressing key challenges in micro-hole blockages, improving aerodynamic performance and ensuring structural reliability.

#### **Keywords:**

HLFC suction panels, electron beam perforation, micro-perforations, TPMS, adhesives.

# 1. Introduction

The aviation sector is actively pursuing technologies that support its commitment to carbon-neutral growth and reduced environmental impact. Among the most effective aerodynamic strategies for reducing drag and improving fuel efficiency is Hybrid Laminar Flow Control (HLFC). HLFC systems maintain laminar flow over aircraft surfaces by drawing in boundary layer air through micro-perforated suction panels, thus delaying transition to turbulent flow and reducing skin-friction drag  $[\underline{1},\underline{2}]$ . This reduction can translate into up to 8-12% fuel savings over long-haul operations, depending on configuration and flight conditions  $[\underline{3}]$ .

A typical HLFC suction panel in the differential design concept for the manufacturing consists of a micro-perforated metallic suction sheet bonded to a lightweight core structure. The core can be realized using various geometric topologies, such as honeycomb, foam, or Triply Periodic Minimal Surface (TPMS) structures. TPMS cores have recently gained interest for their superior isotropic stiffness, energy absorption capacity, and manufacturability via

additive processes [4, 5]. However, despite the aerodynamic promise of HLFC systems, their practical implementation is limited by several manufacturing challenges, most notably, micro-hole blockage during bonding and thermal degradation during perforation.

#### 1.1 Manufacturing challenges in HLFC panel fabrication

In conventional manufacturing, micro-perforations are typically created via laser drilling followed by adhesive bonding to the core structure. When the bonding adhesive is applied after perforation regardless of the drilling process employed, adhesive flow into micro-holes during joining and curing blocks the air flow, reducing suction performance [6]. On the contrary, if laser drilling is performed after adhesive application, the thermal energy from the laser can degrade the adhesive film, cause localized residual stresses or lead to delamination at the bonding interface [7]. To overcome these limitations, this study proposes an alternative manufacturing approach using Electron Beam (EB) drilling on metallic facesheets pre-coated with aerospace-grade adhesive films. EB drilling is a high-precision, high-speed process that generates significantly lower thermal loads compared to laser drilling. By focusing a beam of high-energy electrons onto the target surface in a vacuum environment, material is vaporized in a highly localized region with minimal heat-affected zone [8, 9].

# 1.2 Scope and objectives of this study

This work investigates the feasibility of electron beam perforation for producing HLFC suction panels with metallic facesheets pre-coated with structural adhesives. An aerospace-qualified adhesive film AF 163-2 scotch weld by 3M has already been examined and characterized in terms of tensile and peel strength in a previous study carried out under the scope of this project by Athar et al [23]. A second adhesive film, namely FM 94.03 by Cytec has also been considered and used as a reference as it is already in application at big aerospace research units. Athar et al. also investigated the performance of adhesively bonded sandwich panels under compression loading wherein, 50 x 50 mm stainless steel specimens were bonded by two different adhesive films to three TPMS structures namely gyroid, primitive and diamond. On the basis of these tests, the adhesive film FM 94.03 which showed a better load bearing capacity and gyroid TPMS structure which showed a better structural integrity in the material combination. However, both the adhesive films are considered for further analysis.

In this study, the stainless steel (SS) facesheets are first coated with the adhesive films and lamination is carried out in an autoclave or a heated oven to fix the adhesive layer. They are then subjected to EB perforation under optimized process parameters to generate clean, uniformly distributed micro-holes.

Post-drilling, the SS facesheets are cut into specimens in the required dimensions and bonded to the gyroid TPMS specimen. Before joining, it has to be made sure that the micro perforations remain unblocked at all times; during and after joining. For this purpose, a photoresist material curing at room temperature is applied on to the perforated surface. This material flows into the micro-perforations, cures and blocks them making sure that no adhesive flows into the micro-perforations during joining. The assembled panels are then cured in a second oven step under the curing conditions of the adhesive followed by the removal of photoresist material using acetone and photoresist remover. The sandwich panels are evaluated using the following suite of tests:

- Measurement of hardness of adhesive around the perforations using micro-indenter.
- Scanning Electron Microscopy (SEM) to assess hole integrity, morphology and blockage.

#### 1.3 Significance and novelty

The novelty of this approach lies in the pre-application of adhesives, that is the lamination of metallic face sheets with adhesive films prior to EB perforation, which eliminates the sequential bonding-drilling issues that typically hinders HLFC panel production. This method minimizes micro-hole blockage, preserves adhesive integrity, and enables scalable manufacturing of highly functional HLFC panels. The use of TPMS cores further enhances structural performance while keeping weight low, which is vital for aerospace applications.

Ultimately, this research contributes to the development of manufacturing solutions aligned with aerodynamic optimization and environmental sustainability, supporting the broader goal of achieving next-generation fuel-efficient aircraft.

#### 2. State of the art

# 2.1 Conventional micro-perforation techniques

The industry-level manufacturing of micro-perforated metallic suction sheet remains one of the critical bottlenecks for implementing Hybrid Laminar Flow Control (HLFC) technology in the aviation sector. The strict requirement of maintaining clean, precise micro-perforation patterns to enable controlled boundary layer suction demands for drilling techniques with higher accuracy and production rate. Over two decades, various drilling methods have been explored for micro-perforation of metallic suction sheets in HLFC panels, including mechanical drilling, Electrical Discharge Machining (EDM), EB perforation and laser drilling [10]. Among these, laser and EB perforation technologies have emerged as the most viable for industrial-scale applications, particularly for producing large number of closely spaced micro-holes within limited processing time [11].

In prior studies conducted by Stephen et al. [12-13], conventional laser micro-drilling was performed on titanium (Ti, Grade 2) sheets with dimensions of 200 x 200 x 0.8 mm, employing two distinct techniques: Percussion Micro Drilling (PMD) and Single Pulse Micro Drilling (SPMD). These processes utilized a solid-state pulsed fiber laser with a wavelength of 1065 nm, a maximum power output of 200 W, and pulse frequencies up to 1000 kHz. Both techniques were conducted in the presence of shielding gas, which provided an inert atmosphere and effectively reduced thermal effects during drilling. PMD and SPMD successfully achieved high processing rate of up to 300 holes per second, producing micro holes with diameters ranging from 50-60 µm, owing to high pulse repetition rates and precise laser beam positioning and a distance of 650 µm between the holes in both the laser drilling techniques. Microscopic imaging, after etching and polishing revealed better microstructural quality of the drilled holes for both methods, thus highlighting their suitability for industry-level applications. The results from Stephen et al. [12, 13] serve as a benchmark in this study, providing a critical reference point for evaluating and comparing the performance of conventional laser drilling techniques against more recent approaches such as electron beam micro-perforation.

# 2.2 Joining techniques for HLFC suction panels

The design of Hybrid Laminar Flow Control (HLFC) demands a lightweight, durable bond without micro-holes blockage between the lightweight core structure and the micro-perforated metallic outer skin to ensure effective airflow management. Several joining techniques including welding, brazing, superplastic diffusion bonding, mechanical fastening and adhesive bonding have been explored in aerospace manufacturing over the years.

A detailed comparison between the different joining methods was performed by Humphreys et al. [14]. Among the traditional approaches, techniques like brazing and welding are advantageous for producing narrow plenum chambers with minimal hole blockage, crucial for enhanced suction performance. These methods, however, require both the outer skin and the core structure to be of the same material, thus increasing the overall weight of the system. Furthermore, these joining methods can lead to heat-induced distortion and residual stresses in the thin skin panels, compromising the strength and structural integrity of the panels. Superplastic forming and diffusion bonding offer the potential to fabricate lightweight, integrally bonded structures with minimal obstruction to airflow. However, this method comes with high development costs and design constraints, such as limitations on the width of plenum chambers, which reduce flexibility in structural design. Although mechanical fastening or riveting methods enable efficient joining of metallic components, particularly in applications requiring higher structural rigidity, they introduce mechanical complexity and a potential rise in the weight of the structure.

In contrast to these techniques, adhesive bonding stands out as an attractive alternative due to its weight-saving potential, ability to join dissimilar materials and capability for even load distribution across the bonding surface. Investigations by R. Iwa'nkowicz [15] have demonstrated the merits of adhesive bonding allowing the fabrication of hybrid metal-composite or metal-metal assemblies without introducing significant localized stresses as in case of mechanical fastening or requiring high-temperature processing such as in brazing or welding methods, thus preserving the integrity of the micro-perforated skin. Notwithstanding these advantages, the method still requires precise control over surface treatment, curing parameters and proper adhesive application to ensure high bond strength and consistent performance. Adhesive joints being highly sensitive to environmental variations including change in temperature, humidity or impact loads, the method poses a potential risk of debonding or delamination failure, thus compromising structural integrity and durability of the bond over time.

Although no single joining method addresses all the complexities of HLFC panel construction, adhesive bonding offers a unique balance of lightweight design, compatibility with dissimilar materials and flexibility in manufacturing. However, to fully exploit its advantages, critical challenges such as blockage due to adhesive flow into micro-holes, thermal degradation during post-drilling and environmental durability must be systematically addressed.

## 2.3 TPMS as core structures in HLFC suction panels

Core materials provide a lightweight, low-density intermediate layer to the sandwich panels, adding to the panel's overall thickness with minimal weight. They serve the key mechanical functions such as maintaining separation between the two facesheets, absorbing shear forces and uniformly distributing applied loads, thus improving the shear load-bearing capacity and buckling resistance of the panel [16].

Recently, the mathematically defined TPMS lattice structures have emerged as promising core materials featuring zero mean curvature and a node-free architecture, resulting in more uniform stress distribution and enhanced mechanical performance. Their geometric flexibility enables the design of TPMS cores to be highly customized for specific applications. Their porous, shell-like architecture includes interconnected voids that support removal of debris or excess materials, heat dissipation as well as more internal airflow, making them particularly well-suited for energy-efficient HLFC suction panels [17-19]. These features not only maintain low weight and high stiffness but also enable internal suction pathways essential for improved HLFC function [20].

Among classical TPMS structures, core types such as Primitive, Diamond and Gyroid shown in the <u>Figure 1</u>, have demonstrated superior mechanical capabilities compared to conventional strut-based designs [21]. Recent studies have shown that the topology of TPMS structures significantly influences their mechanical performance. Specifically, the Diamond structure exhibits the highest compressive strength and specific energy absorption, followed by the Gyroid and then the Primitive structures [17, 22]. In the previous study carried out under the scope of this project, these three TPMS structures were additively manufactured by 3D printing using Stereolithography (SLA) and characterized for their mechanical strength under compression loadings [23].

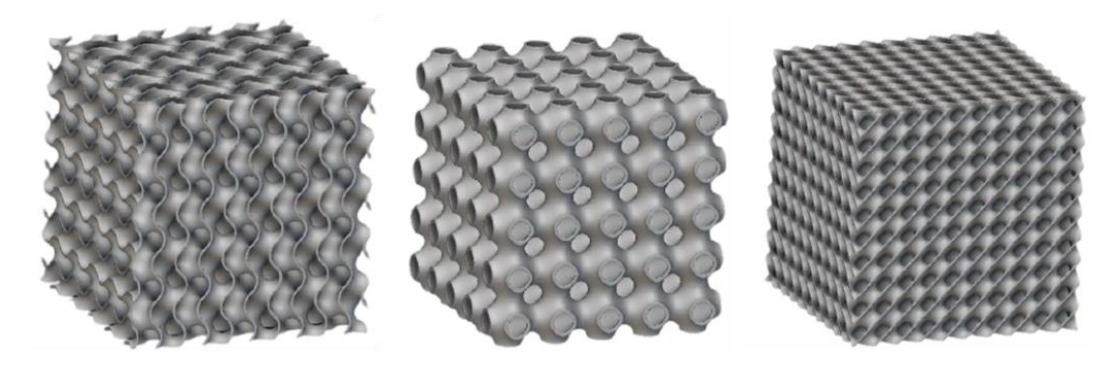


Figure 1: CAD renderings of gyroid, primitive and diamond TPMS

## 2.4 Previously conducted investigations

#### Adhesive characterization

In a previous study by Athar et al. [23], the adhesive performance of 3M Scotch-Weld AF163-2 was evaluated for bonding EB-drilled micro-perforated metallic suction sheets to TPMS lattice cores in HLFC sandwich panels. The adhesive was compared with the aerospace grade adhesive film Cytec FM 94.03 to assess its mechanical properties and bonding effectiveness. Standardized tests including tensile, Mode-I peel (DCB), and compression tests revealed that AF163-2 exhibited high tensile strength, good bond integrity, and stable crack propagation. While FM 94.03 showed slightly higher load-bearing capacity in compression, both adhesives demonstrated excellent bonding performance without delamination or core damage. The findings support the use of both adhesives for reliable integration in HLFC panel manufacturing.

# Microscopic analysis on microperforated SS sheets without adhesive coating

As described in Athar et al. [23], initially the SS specimens with dimensions 100x100x0.6 mm were micro-perforated, without prior application of any adhesive, using a triangular hole pattern with a hole diameter of  $60 \mu m$  and a hole pitch of 10 times the hole diameter ( $10xd_0$ ) i.e.  $600 \mu m$ . Three distinct perforation techniques were employed for this purpose: (1) laser drilling without shielding gas, (2) laser drilling with shielding gas and (3) electron beam perforation. The results from the Scanning Electron Microscopic (SEM) analysis obtained from the different perforation techniques were compared with the benchmark data from Stephen et al. [12, 13], enabling a comprehensive evaluation of the micro-perforation quality as well as exploring the applicability of Electron Beam (EB) drilling as a promising alternative [23].

While laser drilling was initially investigated using both shielded and unshielded conditions, the resulting perforation quality did not entirely meet the desired standards when compared to the benchmark results particularly without the shielding gas where a lot of dirt and debris was observed on the surface. Although Stephen's work described in section 2.1 demonstrated the high efficiency of laser-based methods such as PMD and SPMD, certain limitations such as thermal damage leading to surface quality degradation or heat affected zones (HAZ) regions were still evident in the microscopic analysis [12]. In light of these shortcomings, laser drilling may not be considered as the ideal method and EB drilling is recommended for this intended application. It was further evident that electron beam (EB) perforation of SS sheets, when followed by subsequent etching and deburring, resulted in superior surface quality and more refined perforation morphology compared to the PMD and SPMD laser drilling methods examined in prior studies. Given its significantly higher processing speed, improved surface finish, precise hole geometry, and minimal thermal or mechanical damage to the substrate, EB perforation was identified as the most suitable technique for micro-perforation in this application [23].

# 3. Experimental analysis

Building upon the preliminary investigations on adhesive characterization and micro-perforation techniques described in previous work, this section presents a systematic experimental procedure for the optimized fabrication of HLFC suction panels. The primary objective is to ensure unblocked micro-perforations and robust bonding of metallic face sheets to TPMS core structures through electron beam (EB) perforation of adhesive-coated stainless steel (SS) sheets. The subsequent subsections outline the individual process steps carried out under the scope of this study, including adhesive film lamination prior to perforation, EB drilling under controlled conditions, micro-indentation testing to evaluate adhesive curing, temporary sealing of perforations using photoresist, sandwich panel fabrication, removal of sealing material, and SEM-based microscopic analysis. These experiments collectively assess the feasibility and performance of the proposed manufacturing approach for structurally reliable and aerodynamically functional HLFC panels.

## 3.1 Laminating SS sheets with adhesive films prior to perforation

Following the prior characterization of the adhesive films in terms of their mechanical strength and bonding performance, the subsequent step in this study involved the lamination of stainless-steel (SS) face sheets with adhesive films prior to electron beam (EB) drilling. For this purpose, SS sheets with dimensions of 1 x 0.5 m and thicknesses of 0.6 mm and 0.8 mm were selected. The adhesive films, AF 163.2 and FM 94.03 were applied to the SS sheets manually with assistance from a mechanical squeegee and rollers to ensure uniform distribution and surface conformity.

According to the technical datasheets provided by the manufacturers, the adhesive films require a lamination temperature of 60 °C to achieve sufficient tack and surface wetting prior to full curing. To comply with these parameters, the adhesive-coated stainless-steel sheets were subsequently placed inside a preheated convection oven (see Figure 2) and maintained under a temperature of 60 °C for a duration of 30 minutes. This thermal exposure facilitated the initial softening and wetting of the adhesive layer, promoting intimate contact with the metallic substrate. Upon completion of the lamination cycle, the sheets were carefully removed from the oven and allowed to cool under ambient laboratory conditions. This controlled cooling step is essential to prevent residual thermal stresses and to stabilize the laminated assembly prior to EB perforation.





Figure 2: Lamination of SS sheets with adhesive film in an oven

During the initial lamination trials, as illustrated in <u>Figure 2</u>, the presence of air bubbles was observed on the surface of the adhesive films. Upon closer inspection and systematic visual monitoring, it was determined that these bubbles

were confined to the interface between the adhesive layer and its protective liner. Since the protective film is removed prior to the bonding of the laminated sheet with the core structure, these trapped air pockets posed no risk to the adhesion quality or structural integrity of the final assembly. However, to further enhance the uniformity of lamination and eliminate potential variables associated with manual application and ambient environment, the subsequent lamination procedure was performed under vacuum-assisted conditions within an autoclave system. The same lamination parameters were maintained, i.e., a temperature of 60 °C and a dwell time of 30 minutes to ensure consistency with earlier trials. This setup, depicted in Figure 3, allowed for a more controlled and isolated environment, potentially reducing any inconsistencies introduced by manual handling,

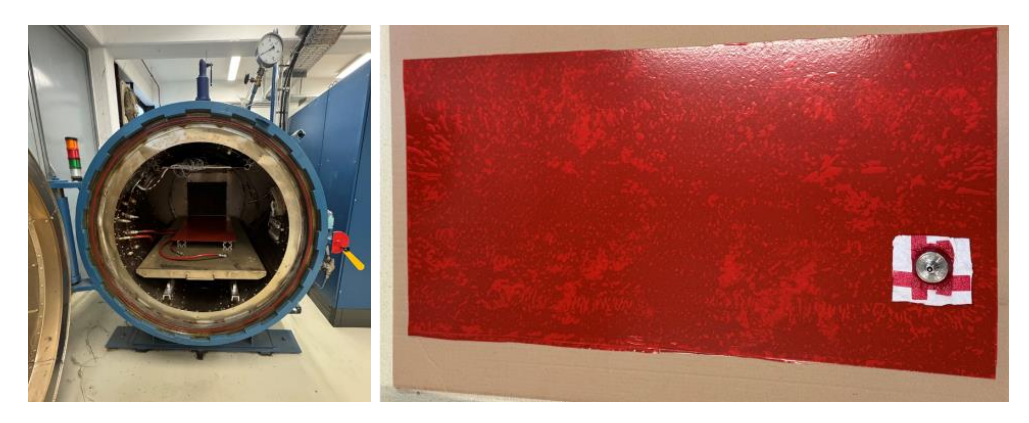


Figure 3: Lamination of SS sheets with adhesive film in an autoclave

Following the vacuum lamination process, the laminated sheets were visually indistinguishable from those prepared under ambient conditions. Notably, the same superficial air bubbles were still present between the adhesive film and its protective liner, reaffirming that their occurrence was unrelated to the bonding interface and thus inconsequential to subsequent process steps. These findings were further corroborated during electron beam perforation and core bonding, wherein no adverse effects such as void formation, delamination, or compromised perforation quality were observed.

Overall, while vacuum lamination offered a cleaner and more controlled processing route, the initial manual method was also deemed sufficiently robust for the given application, provided the protective liner was appropriately removed prior to bonding. These insights highlight the importance of distinguishing between superficial and interface-level defects in laminated assemblies and confirm the reliability of both lamination techniques within the scope of this study. This pre-lamination approach ensures that the subsequent EB perforation process penetrates both the metallic and adhesive layers simultaneously, thus preserving the open-cell structure of the micro-perforations and eliminating the need for post-drilling cleaning or rework. To ensure high-quality bonding and prevent air entrapment either between the layers or within the adhesive matrix, a more controlled and isolated joining environment is essential. In this context, the use of an autoclave provides an optimal solution by enabling vacuum-assisted consolidation under elevated temperature and pressure. Consequently, the fabrication of the sandwich panels in this study was conducted within an autoclave chamber to achieve uniform bonding, eliminate voids, and ensure structural integrity across the adhesive interfaces.

# 3.2 EB perforation on adhesive coated SS sheets

The electron beam drilling process was conducted at ProBeam GmbH using a high-vacuum, precision-controlled system named PK 20 optimized for micro-perforation of thin metallic materials with the process and parameters described in <u>Table 1</u>. In this setup, stainless steel (SS) sheets pre-coated with AF 163-2 structural adhesive film along with the protection film were mounted onto full metal cylindrical fixtures to ensure flatness, stability, and accurate alignment during the perforation. The drilling was carried out with a focused electron beam capable of achieving high drilling speeds and minimal thermal impact, targeting nominal hole diameters of 60-120 µm by locally melting and vaporizing the metal. The vacuumed environment enabled clean beam propagation with minimal scattering, ensuring precise hole morphology with tight tolerances and minimal thermal damage to the surrounding adhesive or substrate.

PK 20 specifications	Value with units
Chamber volume	$2 \text{ m}^3$
Maximum voltage	120 kV
Beam power	3 kW
Perforation speed	2000 holes per second

Table 1. EB perforation machine specifications

To investigate the influence of adhesive positioning on perforation quality and potential hole blockage, two configurations were prepared: in one case, the adhesive film was applied on the outer side of the SS sheet, directly exposed to the beam, while in the other, it was placed on the inner side, shielded from the beam. This variation allowed for a comparative analysis of drilling behavior through adhesive layers and its impact on hole morphology. After the drilling process, all sheets underwent a post-treatment phase, which included cleaning to remove vaporized residue and particle deposits, followed by surface grinding to ensure uniformity and restore bonding surface quality for subsequent joining to TPMS core structures.

After the electron beam drilling process, it was observed that specimens with the adhesive film placed on the outer side, directly facing the beam, exhibited prominent brown discoloration on the surface even after subsequent cleaning and grinding. This discoloration is likely due to the thermal degradation or burning of the adhesive's protective film when exposed directly to the high-energy beam. In contrast, no such browning was observed in the configuration where the adhesive was on the inner side, i.e., shielded from the beam by the stainless-steel sheet as shown in Figure 4. As a result, further investigation was required specifically for the outer-side configuration to assess whether the adhesive itself was thermally damaged or altered during the drilling process.



Figure 4: EB perforated SS sheet with adhesive on outer side (left) and adhesive on the inner side (right)

In addition to potential burning, if any, it was necessary to evaluate the degree of curing (by determining the hardness) of the adhesive film induced by the thermal load from electron beam exposure. For this purpose, micro-indentation was carried out on the adhesive film after EB drilling in the affected regions i.e., the regions around the micro-perforations, as detailed in the following section. For comparison and determining the extent to which EB drilling cured the adhesive film during the process, the micro-indentation was also carried out on the uncured adhesive specimens. Furthermore, microscopic analysis using scanning electron microscopy (SEM) was essential at multiple stages: prior to joining, after photo resist application, after bonding and removal of the photo resist material. These SEM evaluations, as outlined in Section 3.6, provided detailed insight into the structural integrity, surface condition, and any microstructural changes induced during the perforation and joining processes.

## 3.3 Micro-indentation tests

Micro-indentation tests were conducted using a Fischerscope HM2000 micro-indenter according to ISO 14577 to evaluate the mechanical properties (Marten's hardness as well as Force-Depth behaviours) of the adhesive film FM 94.03 in both uncured form and around the micro-perforations in the EB perforated sheets as described above. The indentations were specifically targeted in the adhesive regions surrounding the EB-induced perforation holes to

investigate localized mechanical property changes and the extent to which the adhesive is cured during the process. For this purpose, the uncured adhesive as well as the EB perforated specimens in the dimension 100 x 34 mm were mounted on a metallic fixture as shown in <u>Figure 5</u> to ensure parallelism of the surface which is really important for indentation. This fixture is then kept under the microscope attached to the micro-indenter as shown in <u>Figure 6</u> to determine and select the points for indentation.

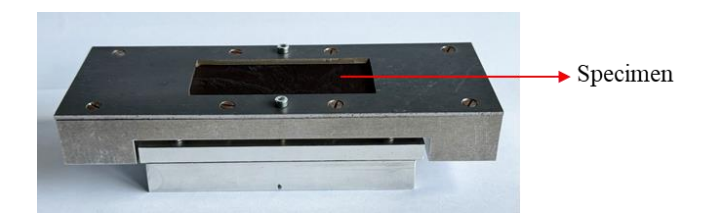


Figure 5: Metallic fixture for mounting the specimens

Each indentation was performed with a maximum load of 200 mN, applied over a loading time of 20 seconds followed by unloading over 20 seconds. Around a micro-perforation, 3 points were selected for indentation and measurement of force versus depth curves in order to assess whether the electron beam exposure, used for perforating metal sheets in HLFC (Hybrid Laminar Flow Control) panels, induces any degree of curing in the adhesive, which could affect its bonding performance.



Figure 6: Fischerscope HM2000 microindenter (left), attached microscope (middle) and the micro-indenter (right)

From the indentation tests, the force vs depth curves were obtained for both; the uncured adhesive as well as the adhesive around the micro-perforations as shown in <u>Figure 7</u>.

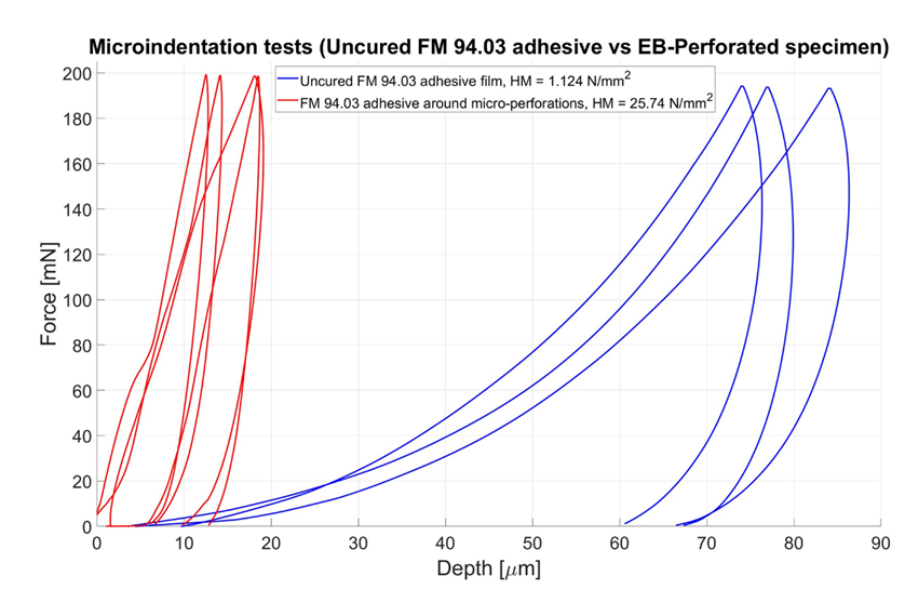


Figure 7: Results from the micro-indentation tests for uncured adhesive and EB perforated specimen

In this diagram shown above, the blue curves correspond to the uncured FM 94.03 adhesive film. These curves show a gradual and smooth increase in indentation force with increasing penetration depth, reaching up to approximately 80 µm. This behavior is characteristic of a soft, uncured polymeric adhesive with low mechanical resistance. The calculated Marten's hardness (HM) for the uncured adhesive is relatively low, at 1.124 N/mm² i.e. the material offers minimal resistance to indentation. In contrast, the red curves represent the FM 94.03 adhesive material located around the electron beam-drilled micro-perforations. These curves show a significantly steeper rise in indentation force with increasing depth and achieve similar peak forces at significantly lower depths i.e. less than 20 µm in most cases. The stiffness and resistance to penetration suggest that the adhesive in this region has undergone substantial curing or crosslinking, likely due to localized thermal or radiative energy input during the EB drilling process. This is further supported by the higher hardness modulus of 25.74 N/mm², which is over 20 times greater than that of the uncured adhesive. However, this is yet to be confirmed using chemical and thermal analysis such as FTIR or DSC which was carried out under the scope of this study. In the diagram, it can also be seen that the curves for 3 different points of one specimen do not exactly coincide with each other which is due to the non-parallel surfaces around the measuring points.

# 3.4 Photoresist application for temporary sealing of micro-perforations

As outlined previously, the application of a photoresist layer serves to temporarily seal the micro-perforations during the adhesion or joining process, thereby preventing the flow of adhesive material into the perforation channels. Following bonding, the photoresist is subsequently removed to restore the open-state permeability of the micro-perforated regions. Under the scope of this study, the process of photoresist application comprised the following three steps:

#### Coating and initial drying

The perforated specimens were cut in the dimension 100x100 mm and a thin and uniform layer of photoresist was applied onto the pre-cleaned surface of the micro-perforated specimens using a roller squeegee to ensure homogeneous application across the surface. The specimens were then subjected to an initial drying phase using a hand-held hot air blower for approximately 5 minutes until the surface attained a matte and smooth appearance as illustrated in Figure 8. To allow further solvent evaporation and preliminary stabilization of the photoresist film, the specimens were placed in a dark environment for approximately one hour.



Figure 8: Coating and drying of photoresist layer on EB-perforated specimen

#### Curing

Curing is a critical step to ensure that no residual uncured photoresist remains on the surface or within the microperforations. The photoresist used in this study cures effectively under ultraviolet (UV) light or direct sunlight. Accordingly, the specimens were exposed to sunlight for approximately one minute to initiate the crosslinking reaction and achieve sufficient curing of the resist layer.





Figure 9: Specimen kept in darkness for drying (left) and in sunlight for curing (right)

#### **Development and final curing**

A 1 wt% developer solution was prepared by dissolving 10 g of developer powder in 1 liter of water. The specimens were immersed in this solution for 2 minutes to initiate the development process, during which uncured regions of the photoresist were selectively removed. After development (see <u>Figure 10</u>), the specimens were rinsed with cold water for an additional 2 minutes to terminate the development reaction and remove any residual chemicals. The specimens were then dried using a hot air blower.



Figure 10: Development of photoresist; preparation of solution, dipping of coated part in solution and washing

To ensure full polymerization and stability of the remaining cured photoresist, a final curing step was carried out by exposing the specimens again to direct sunlight for 10 minutes.

# 3.5 Fabrication of sandwich panels

Subsequent to the application of the photoresist material, which serves to temporarily blocks the micro-perforations, the next phase of this investigation involved the fabrication of sandwich specimens. For this purpose, SS face sheets measuring 100x100 mm and featuring through-thickness micro-perforations as well as pre-applied perforated adhesive film were assembled with an additively manufactured gyroid core structure. The gyroid specimen as shown in the Figure 11 was produced via 3D printing using SLA technique using inverted SLA 3D printer Elegoo Mars 2 followed by soaking in water bath for 5 mins and UV-curing for mins, and had dimensions of 100x100x20 mm.



Figure 11: 3D printed gyroid structure for HLFC suction panel

During assembly, clips were employed at the lateral edges of the stack to constrain any relative movement between the layers and to maintain alignment during the thermal bonding process. The assembled specimens were then transferred to a convection oven and subjected to a temperature of 120 °C for one hour, consistent with the recommended curing conditions of the adhesive film used (<u>Figure 12</u>) after which, the specimens were removed from the oven and allowed to cool to ambient temperature.



Figure 12: Adhesively bonded HLFC suction panel specimen (right)

#### Stripping off photoresist from the surface and micro-perforations

Following the bonding process, it was necessary to remove the photoresist from both the surface of the SS sheet and the micro-perforations to ensure unobstructed suction flow and maintain surface integrity. For this purpose, a 10 wt% developer solution was prepared by dissolving 50 g of the developer in 450 ml of hot water and the sandwich panel was dipped in this solution upside down as shown in the Figure 13 below:

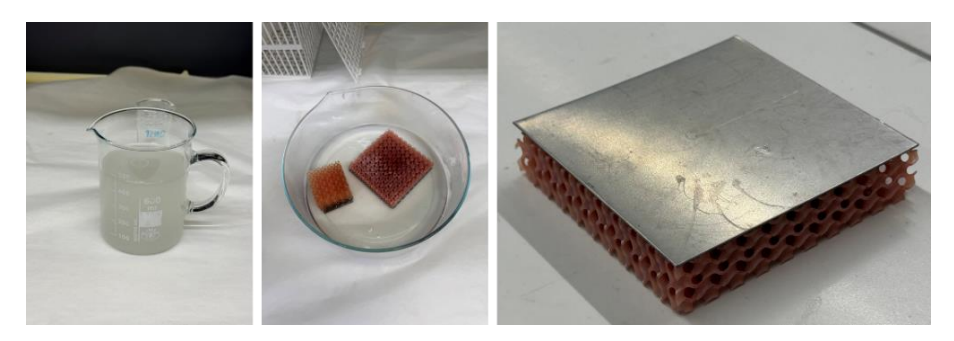


Figure 13: Stripping off photoresist from the sandwich panel

The photoresist layer begins to dissolve readily upon immersion in the developer solution and detaches from the surface within approximately one minute. Any remaining residue was gently removed using a fine glazing paper to avoid damaging the perforated structure. Subsequently, the surface was cleaned with a lint-free tissue to eliminate any loose particles or solvent residues. This procedure ensures a clean and fully open microperforated surface, which is critical for the aerodynamic functionality of the HLFC suction panel.

# 3.6 Microscopic analysis of adhesive coated and EB perforated SS sheets

After stripping off the photoresist material, the sandwich panel specimens were examined using an in-house FEI Quanta 650 FEG Scanning Electron Microscope (SEM). Imaging was conducted at varying under high vacuum (HiVac) conditions with an accelerating voltage of 30 kV. The Everhart-Thornley Detector (ETD) was utilized to capture both secondary and backscattered electrons. The acquired micrographs were displayed with a defined horizontal field of view (HFW) on the computer system connected to the SEM for further analysis. As outlined in the previous sections, microscopic analyses were performed at multiple critical stages of the process: immediately after electron beam perforation and prior to bonding, following the application of the photoresist, and subsequently after the complete fabrication of the sandwich panels including the removal of the photoresist. These sequential observations enabled a comprehensive evaluation of surface condition, micro-perforation integrity, and potential alterations introduced during each processing step.

# After perforation with pre-applied adhesive:

The first series of microscopic analyses with SEM were performed on the EB-perforated SS sheet specimens with preapplied adhesive wherein the adhesive also got perforated along. For this purpose, 100x100 mm specimens were cut from the bigger sheets perforated and examined under the microscope. The SEM images shown in Figure 14 illustrate the surface condition and micro-perforation quality of the metallic sheet with pre-applied adhesive after electron beam perforation and subsequent grinding and processing steps. As evident from both magnification levels, no blockage of the micro-holes was observed, confirming that the integrity of the perforations remained intact throughout the procedure. The surface appeared cracked though which might indicate the thermal degradation or decomposition of organic components leading to outgasing which might be due to residue of the degraded protection film of the adhesive, however, at this stage of the study, the goal was to achieve unblocked micro-perforations, with regards to which the perforation method and the novel technique of using pre-applied adhesive on SS sheets showed a promising approach. Moreover, it was observed that the adhesive did not flow into the perforations during either the electron beam drilling or the subsequent grinding steps, thereby preserving the open-area ratio essential for the aerodynamic function of the HLFC suction panel.

Figure 14: SEM images of adhesive coated EB perforated SS sheets (steel side)

Microscopic analysis using SEM was also conducted for the adhesive coated side of the sheet, where the adhesive film was oriented outward, i.e., facing the beam during perforation. As seen in the images (see Figure 15), the microperforations appeared unblocked by adhesive, indicating successful perforation through the adhesive coated surface. However, localized surface irregularities and bulging could be observed around the edges of the perforations. These features likely resulted from thermal exposure during EB drilling, potentially causing partial curing or degradation of the adhesive film in those regions. The hardness measurements using micro-indenter, as discussed in Section 3.3, were conducted specifically in these bulged regions around the hole edges to assess the extent of thermally induced curing or property changes in the adhesive due to direct beam exposure.

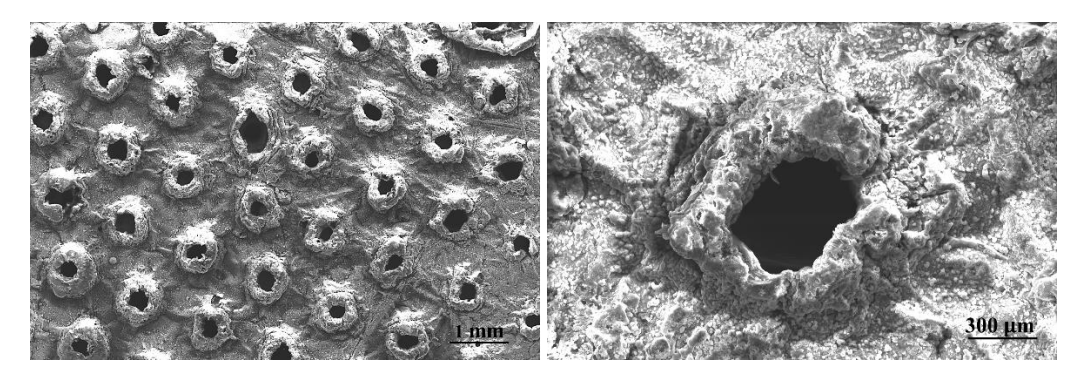


Figure 15: SEM images of adhesive coated EB perforated SS sheets (adhesive side)

# After the application of photoresist material

The SEM images in Figure 16 show the surface morphology of the adhesive coated EB perforated SS sheet after the application of photoresist at different scale and magnification levels. As intended, the micro-perforations appeared to be effectively and uniformly blocked by the photoresist material, indicating successful surface coating. The photoresist temporarily sealed the holes to prevent contamination or adhesive infiltration during subsequent processing steps including joining. This temporary sealing behaviour is a critical part of the process chain, particularly in HLFC panel fabrication, as it preserves the functional open-area ratio by ensuring the holes remain unblocked, by temporarily sealing them until final cleaning. The bright circular zones surrounding the perforations are likely due to contrast variation caused by differences in surface topography between the SS and the resist-coated regions. Additionally, the uniform distribution of the photoresist suggests good surface wetting. These observations confirm that the photoresist application fulfilled its intended function of sealing the micro-perforations, which were removed after the panel fabrication.

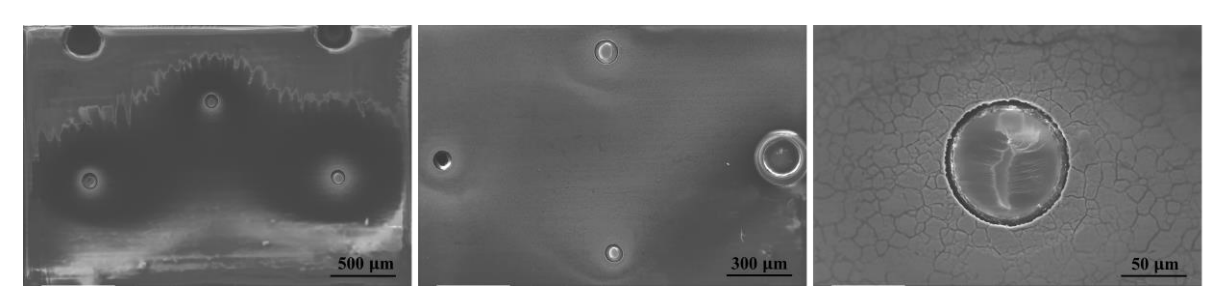


Figure 16: SEM images after photoresist application

#### After fabrication of sandwich panel and stripping-off photoresist

The presented SEM images in Figure 17 show the condition of the perforated SS sheets after the complete fabrication of the sandwich panels and the removal of the photoresist layer. The micro-perforations remained largely open and unobstructed, confirming that the cleaning process was effective and the suction functionality is retained. However, upon closer examination, slight impressions or deformations could be observed within or around several holes. These features were not present in earlier processing stages and are therefore likely a result of the bonding step. One possible cause of these impressions is the direct contact with the TPMS core during joining process. The complex geometry of the TPMS core may have exerted localized pressure on the SS face sheet, leading to surface deformation in areas aligned with the TPMS's structural elements.

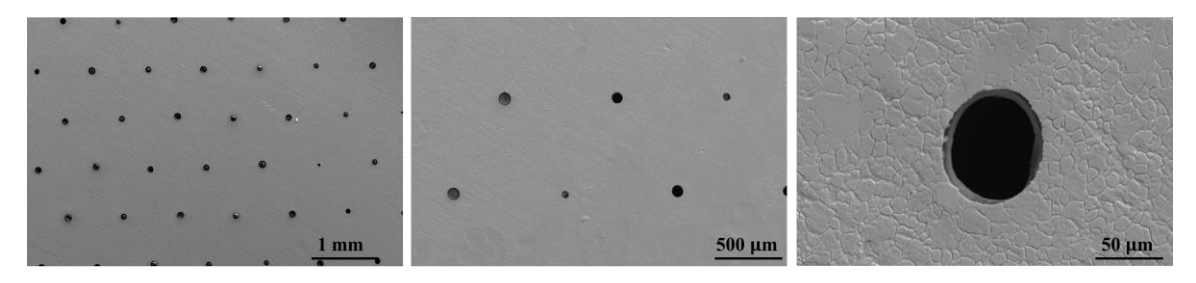


Figure 17: SEM images after panel fabrication and photoresist removal

While these impressions do not significantly obstruct the perforations, they may slightly alter the surface texture around the holes, which could influence local airflow characteristics. Further evaluation may be necessary to determine whether these changes impact the aerodynamic performance of the suction panel.

# 4. Summary and outlook

In this study, a novel manufacturing approach for HLFC suction panels was demonstrated, wherein metallic stainless-steel face sheets pre-coated with aerospace-grade adhesive films were micro-perforated using electron beam (EB) drilling and subsequently bonded to additively manufactured Triply Periodic Minimal Surface (TPMS) core structures. The results confirm that the EB perforation process enables precise, thermally controlled drilling through both metal and adhesive layers without compromising the open-area ratio, which is critical for boundary layer suction performance. Microscopic analysis revealed no adhesive intrusion into the perforations during drilling or bonding, and the use of photoresist as a temporary sealing agent was shown to be effective in preserving hole integrity throughout the process chain. Furthermore, micro-indentation tests indicated a significant increase in local hardness of the adhesive surrounding the perforations, suggesting partial curing induced by electron beam exposure, a factor that requires further investigation. While the adhesive pre-application strategy combined with EB perforation proved effective in preventing hole blockage, slight surface alterations were observed post-joining, potentially due to localized interaction with the TPMS core geometry. These impressions, although not obstructive, may have subtle effects on flow uniformity and require further aerodynamic assessment.

In this context, the results presented in this study validate the feasibility and robustness of the employed process chain for HLFC suction panel fabrication. The successful integration of adhesive pre-application, EB drilling, photoresist sealing, and bonding with the TPMS core demonstrates a high level of process compatibility and manufacturing control. The preservation of perforation integrity, absence of adhesive blockage and consistent bonding performance confirm that the methodology meets key functional and structural requirements. These findings highlight the potential of this approach for reliable scale-up and application in effective production of HLFC systems, where both aerodynamic precision and structural reliability are critical.

Looking forward, several key areas remain to be explored to validate and enhance the proposed fabrication methodology. Most notably, flow meter analysis of the fabricated sandwich panels is necessary to quantitatively assess airflow characteristics and validate the findings from SEM imaging. This will help determine whether surface impressions or adhesive curing gradients impact suction uniformity or flow resistance. Additionally, chemical and thermal analyses such as FTIR and DSC should be performed to confirm the extent and uniformity of adhesive curing caused by EB exposure. Finally, optimization of autoclave bonding parameters and potential use of interfacial buffer layers may further improve surface quality and bonding performance. Overall, the integrated method of pre-applied adhesives combined with EB drilling and TPMS core bonding presents a promising path toward scalable, high-performance HLFC panel fabrication, aligning with industry goals for aerodynamic efficiency and sustainable aircraft design.

# 5. Acknowledgements

The results of this paper have been developed within the framework of the project "Bonding technologies for hybrid suction designs" which is a part of the excellence cluster of the Technische Universität Braunschweig called Sustainable Energy Efficient Aviation (SE2A). This project is funded by the German Research Foundation (DFG). The responsibility of the content of this publication lies with the authors.

#### References

- [1] Braslow, A. L. A History of Suction-Type Laminar-Flow Control with Emphasis on Flight Research. NASA, 1999.
- [2] Joslin, R. D. "Overview of Laminar Flow Control." NASA Langley Research Center, 1998.
- [3] Smith, J. W., et al. "Fuel Savings through HLFC on Transport Aircraft." AIAA Journal, vol. 47, no. 5, 2009.
- [4] Maskery, I., et al. "Mechanical Properties of TPMS Structures." Materials Science and Engineering A, 2017.
- [5] Kapfer, S. C., et al. "TPMS Lattices: Geometry and Mechanical Behavior." Acta Materialia, 2011.
- [6] Wei, Y., et al. "Adhesive Blocking of Micro-Perforations in HLFC Panels." Journal of Adhesion Science, 2014.
- [7] Oliveira, J. P., et al. "Residual Stresses from Laser Drilling in Aerospace Materials." Journal of Materials Processing Technology, 2016.
- [8] Russek, U. A., "Advances in Electron Beam Technology for Precision Drilling." Journal of Manufacturing Science, 2020.
- [9] Zhang, Y., et al. "Micro-Drilling of Metal Foils Using E-Beam Techniques." Surface and Coatings Technology, 2018.
- [10] Michel, S., Analysis of the laser drilling process for pilot holes in complex shaped components, Procedia CIRP 74, p. 398, 2018.
- [11] Andreas, S., "High-speed manufacturing of HLFC structures by laser micro drilling" Lasers in Manufacturing Conference, 2019.
- [12] Andreas Stephen, et al. "Laser micro drilling methods for perforation of aircraft suction surfaces", Procedia CIRP, Volume 74, 2018.
- [13] Andreas Stephen, et al. "High Speed Laser Micro Drilling for Aerospace Applications", Procedia CIPR, Volume 24, 2014.
- [14] Humphreys B., "Investigation of hybrid laminar flow control (HLFC) surfaces", Aircraft Design 4, p. 127–146, 2001.
- [15] Iwa'nkowicz, R., et al., "Review of joining methods of sandwich panels in ship construction," volume 3, Jan.
- [16] He L., et al., "Blast resistance in sandwich structures based on tpms", Buildings, volume 13, number 11, 2023.
- [17] Qiu N., et al., Experimental and numerical studies on mechanical proper ties of tpms structures, International Journal of Mechanical Sciences, volume 261, page 108657, 2024.
- [18] Saleh M. et al., Compression performance and failure analysis of 3d printed carbon fiber/pla composite tpms lattice structures, Polymers, volume 14, number 21, 2022.
- [19] Mapari, H. et al., "Effect of residual stresses on the mechanical properties of tpms lattice structures manufactured using 316l stainless steel," Jan. 2023.
- [20] Wiedemann et al., The Suction Panel -xHLFC and Structural Solution for Energy Efficient Aviation. 10.2514/6.2022-0007, 2021.
- [21] Qureshi Z. A. et al., Thermal characterization of 3d-printed lattices based on triply periodic minimal surfaces embedded with organic phase change material, Case Studies in Thermal Engineering, volume 27, 2021.
- [22] Novak N. et al., Quasi-static and dynamic compressive behaviour of sheet tpms cellular structures, Composite Structures, volume 266, page 113801, 2021.
- [23] Athar. et al., "A Novel Technique to Join Electron Beam Perforated Metallic Sheets to Core Structures in the Design of Hybrid Laminar Flow Control Suction Panels", Available at SSRN 5197550.